

Research Article



Received: Dec 9, 2022

Revised: Feb 24, 2023

Accepted: Feb 24, 2023

Published online: Apr 27, 2023

Lagos de Melo LP, Queiroz PM, Moreira-Souza L, Nadaes MR, Santaella GM, Oliveira ML, Freitas DQ

*Correspondence to

Larissa Pereira Lagos de Melo, DDS, MSc, PhD

Department of Oral Diagnosis, Division of Oral Radiology, Piracicaba Dental School, University of Campinas, Piracicaba, Av. Limeira, 901, SP 13414-903, Brazil.

Email: melo.lpl@gmail.com

Copyright © 2023. The Korean Academy of Conservative Dentistry

This is an Open Access article distributed under the terms of the Creative Commons Attribution Non-Commercial License (<https://creativecommons.org/licenses/by-nc/4.0/>) which permits unrestricted non-commercial use, distribution, and reproduction in any medium, provided the original work is properly cited.

Funding

This study was partially supported by CAPES (Coordenação de Aperfeiçoamento de Pessoal de Nível Superior - Brazil) - Finance code 001.

Conflict of Interest

No potential conflict of interest relevant to this article was reported.

Author Contributions

Conceptualization: Lagos de Melo LP, Queiroz PM, Freitas DQ. Data curation: Lagos de

Influence of CBCT parameters on image quality and the diagnosis of vertical root fractures in teeth with metallic posts: an *ex vivo* study

Larissa Pereira Lagos de Melo ,^{1,*} Polyane Mazucatto Queiroz ,¹
Larissa Moreira-Souza ,¹ Mariana Rocha Nadaes ,² Gustavo Machado Santaella ,³
Matheus Lima Oliveira ,¹ Deborah Queiroz Freitas ¹

¹Department of Oral Diagnosis, Division of Oral Radiology, Piracicaba Dental School, University of Campinas, Piracicaba, São Paulo, Brazil

²Dental Clinic Department, Division of Oral Radiology, Dental School, Federal Fluminense University, Niterói, Rio de Janeiro, Brazil

³Department of Diagnosis and Oral Health, University of Louisville, School of Dentistry, Louisville, KY, USA

ABSTRACT

Objectives: The aim of this study was to evaluate the influence of peak kilovoltage (kVp) and a metal artifact reduction (MAR) tool on image quality and the diagnosis of vertical root fracture (VRF) in cone-beam computed tomography (CBCT).

Materials and Methods: Twenty single-rooted human teeth filled with an intracanal metal post were divided into 2 groups: control ($n = 10$) and VRF ($n = 10$). Each tooth was placed into the socket of a dry mandible, and CBCT scans were acquired using a Picasso Trio varying the kVp (70, 80, 90, or 99), and the use of MAR (with or without). The examinations were assessed by 5 examiners for the diagnosis of VRF using a 5-point scale. A subjective evaluation of the expression of artifacts was done by comparing random axial images of the studied protocols. The results of the diagnoses were analyzed using 2-way analysis of variance and the Tukey *post hoc* test, the subjective evaluations were compared using the Friedman test, and intra-examiner reproducibility was evaluated using the weighted kappa test ($\alpha = 5\%$).

Results: The kVp and MAR did not influence the diagnosis of VRF ($p > 0.05$). According to the subjective classification, the 99 kVp protocol with MAR demonstrated the least expression of artifacts, while the 70 kVp protocol without MAR led to the most artifacts.

Conclusions: Protocols with higher kVp combined with MAR improved the image quality of CBCT examinations. However, those factors did not lead to an improvement in the diagnosis of VRF.

Keywords: Artifacts; Cone-beam computed tomography; Diagnostic imaging; Vertical root fracture

INTRODUCTION

A vertical root fracture (VRF) is defined as an interruption of the dental tissue that extends longitudinally along the root of a tooth [1]. The diagnosis of VRF can often be complex

Melo LP, Moreira-Souza L, Freitas DQ. Formal analysis: Lagos de Melo LP, Santaella GM, Nadaes MR, Freitas DQ. Funding acquisition: Lagos de Melo LP, Freitas DQ. Investigation: Lagos de Melo LP, Freitas DQ. Methodology: Lagos de Melo LP, Moreira-Souza L, Queiroz PM, Freitas DQ. Project administration: Lagos de Melo LP, Freitas DQ. Resources: Lagos de Melo LP, Freitas DQ. Software: Lagos de Melo LP, Santaella GM, Nadaes MR. Supervision: Lagos de Melo LP, Oliveira ML, Freitas DQ. Validation: Lagos de Melo LP, Freitas DQ. Visualization: Lagos de Melo LP, Queiroz PM, Moreira-Souza L, Nadaes MR, Santaella GM, Oliveira ML, Freitas DQ. Writing - original draft: Lagos de Melo LP, Freitas DQ. Writing - review & editing: Lagos de Melo LP, Queiroz PM, Santaella GM, Nadaes MR, Oliveira ML, Freitas DQ.

ORCID iDs

Larissa Pereira Lagos de Melo 
<https://orcid.org/0000-0001-6687-5684>
Polyane Mazucatto Queiroz 
<https://orcid.org/0000-0001-7324-7838>
Larissa Moreira-Souza 
<https://orcid.org/0000-0002-6722-3183>
Mariana Rocha Nadaes 
<https://orcid.org/0000-0001-6652-9933>
Gustavo Machado Santaella 
<https://orcid.org/0000-0002-0884-2443>
Matheus Lima Oliveira 
<https://orcid.org/0000-0002-8054-8759>
Deborah Queiroz Freitas 
<https://orcid.org/0000-0002-1425-5966>

because it presents with nonspecific clinical findings. However, a proper diagnosis is crucial to avoid unnecessary extraction of an otherwise treatable tooth [2,3].

Imaging examinations are essential for the diagnosis of VRF. Cone-beam computed tomography (CBCT) is particularly useful for this purpose since it eliminates the anatomical overlap present on radiographs, preventing the fracture from being masked by the tooth and adjacent structures, which occurs when the X-ray beam is not parallel to the fracture line [1,4].

However, despite the several advantages of CBCT, when metallic materials are present in the oral cavity, such as intracanal posts, the diagnosis of VRF becomes complicated due to the formation of artifacts in the image [3]. Artifacts are errors in recording the data that produce distorted images, which do not correspond to the real object and consequently degrade the image quality [5]. Artifacts occur due to the interaction of the X-ray beam with materials of high density and atomic number, and appear as streaks and shadows that arise from the metallic material and overlap with the tooth root; thus, artifacts can make it difficult to visualize a fracture, which can lead to a false-negative result, or even mimic a fracture, which can lead to a false-positive finding [4,6].

Some features have been tested to minimize or even eliminate the negative impact of artifacts on the detection of VRF. One of them is the metal artifact reduction (MAR) algorithm available in some CBCT units. MAR works by reducing the variability of gray values, increasing the contrast-to-noise ratio, and improving image quality when objectively evaluated [6-9]. However, it has not yet been determined that MAR improves the accuracy of VRF diagnoses in clinical settings [9-11], suggesting that other methods to improve diagnostic accuracy are needed.

In addition to the MAR tool, increasing the peak kilovoltage (kVp) can also reduce the expression of metal artifacts [12], as has been shown in objective analyses [13-15]. However, this evidence obtained through objective assessments does not directly correspond to practical clinical circumstances. Further investigations are needed to understand whether this reduction in metal artifacts is significantly relevant to the diagnosis of VRF. Considering the limited clinical information on the influence of kVp on the reduction of metal artifacts, this study aimed to evaluate the impact of kVp, with or without the MAR tool, on image quality and the diagnosis of VRF in teeth with metallic intracanal posts. The null hypothesis was that kVp and the MAR tool would not influence image quality or the diagnosis of VRF.

MATERIALS AND METHODS

Sample

This study was approved by the local institutional review board (protocol #3268885) and followed the guidelines of the Helsinki Declaration.

Twenty single-rooted human teeth (mandibular canines and premolars) extracted for reasons unrelated to the study were disinfected with 70% alcohol and subjected to scaling and root planning treatment to remove dental calculus and soft tissues. Subsequently, the crowns were sectioned at the cemento-enamel junction to eliminate the identification of coronary fractures. The roots were instrumented using the Mtwo NiTi[®] rotary system (VDW, Munich, Germany). VRFs were induced using a universal testing machine (Instron 4411; Instron

Corporation, Canton, MA, USA) in half of the sampled roots ($n = 10$). For this, each tooth was temporarily placed in an acrylic block with a central opening of 10 mm in diameter. A tapered metal tip was introduced at the entrance of the root canal and, after the fracture occurred, the machine automatically stopped its operation, which produced incomplete fractures (without fragment separation). The absence or presence of fractures was confirmed using transillumination and microscopy.

The samples were divided into 2 groups: without VRF (control; $n = 10$), and with VRF ($n = 10$). In the apical third, a gutta-percha cone with the same diameter and taper as the instrumentation (Dentsply Maillefer, Ballaigues, Switzerland) was added so that the canal was filled in its entire length, but without the use of any endodontic cement so that it would not penetrate the fracture line and facilitate its identification. In the middle and cervical thirds, a cast metal post composed of a cobalt-chromium metal alloy was inserted. The adaptation of the post and gutta-percha cone was confirmed using periapical radiographs.

Image acquisition

For image acquisition, each tooth was inserted into the socket of a missing canine in a dry human mandible, which was enlarged with the aid of a cylindrical bur (KG Sorensen, São Paulo, Brazil). The mandible was fully covered by a 10-mm-thick layer of wax to simulate the attenuation of X-rays by the soft tissues of the maxillofacial region. The exams were acquired using a Picasso Trio unit (Vatech, E-WOO Technology Co, Ltd., Yongin, Korea), which has a pulsating beam and adjustable energy parameters. Thus, each tooth was scanned 8 times, changing the kVp between 70, 80, 90, and 99, with or without the MAR tool. The milliamperage (3.8 mA), the size of the field of view (FOV; 5×5 cm), the voxel size (0.2 mm), and the scanning mode (high resolution, exposure time = 24 seconds; rotation = 360° ; basis images = 720) were fixed in all acquisitions. These acquisition parameters were selected according to the protocol indicated by the device manufacturer for an adult patient using the smallest voxel size. The mandible was positioned in the unit with the occlusal plane parallel to the ground, the mid-sagittal plane perpendicular to the ground, and the FOV centered in the canine region with the aid of the device's aligning guiding lights. In total, 160 scans were acquired (20 teeth \times 4 kVp conditions \times 2 MAR conditions).

Image evaluation

The images were evaluated individually by 5 oral and maxillofacial radiologists with more than 5 years of experience in CBCT after a training session, without prior knowledge of the root condition or the scanning/reconstruction protocols, in a dimmed and quiet room. A 15" FullHD monitor ($1,920 \times 1,080$) was used, and the examiners were allowed to adjust the brightness, contrast, and zoom settings during the evaluations. The examiners were instructed on how to perform all evaluations.

1. Diagnosis of VRF

The examiners assessed the presence of VRF based on a 5-point scale—1) definitely absent, 2) probably absent, 3) uncertain, 4) probably present, and 5) definitely present—on the OnDemand3D™ software (CyberMed, Seoul, Korea) using a dynamic evaluation of the volume.

2. Image quality

The image quality was assessed in 2 ways. First, the 5 examiners rated each exam using a 5-point scale—1) very poor, 2) poor, 3) acceptable, 4) good, and 5) excellent—in the same

sessions in which they performed the diagnosis of VRF on the OnDemand3D™ software (CyberMed) using a dynamic evaluation of the volume.

In other sessions, the examiners received 20 templates made in PowerPoint (Microsoft Corp., Redmond, WA, USA) without compression of the images, and the templates were evaluated in the same software for subjective assessment of the quantity of artifacts. Each template included 8 corrected axial reconstructions, one of each protocol for the same tooth, arranged in a random order. They were instructed to sort the images in an increasing order according to artifact expression, assigning 1 to the image with the least expression of artifacts, and 8 to the image with the most artifacts. The images used in the templates were standardized to be the axial slice corresponding to a distance of 3 mm from the superior limit of the root of each tooth evaluated and to be perpendicular to the root (**Figure 1**). **Figure 2** shows an example of a template. After 15 days, all evaluations were repeated for 20% of the sample under the same conditions to assess intra-examiner reproducibility.

Statistical analysis

All analyses were performed using SPSS version 23.0 (IBM Corp., Armonk, NY, USA) and GraphPad Prism 6.0 (GraphPad Software, La Jolla, CA, USA), with a significance level of 5%. The power of the analyses was 80%, considering a minimal difference among the groups, the mean and standard deviation, and the number of repetitions per group. The effect size was moderate.

For the diagnosis of VRF, the diagnostic performance (area under the receiver operating characteristic [ROC] curve, sensitivity, and specificity) for each protocol and each examiner were calculated, and the results were compared using 2-way analysis of variance and the Tukey *post hoc* test to evaluate the influence of kVp, MAR, and the interaction between them on the detection of VRF. The results were expressed as mean and standard deviation values for each protocol.

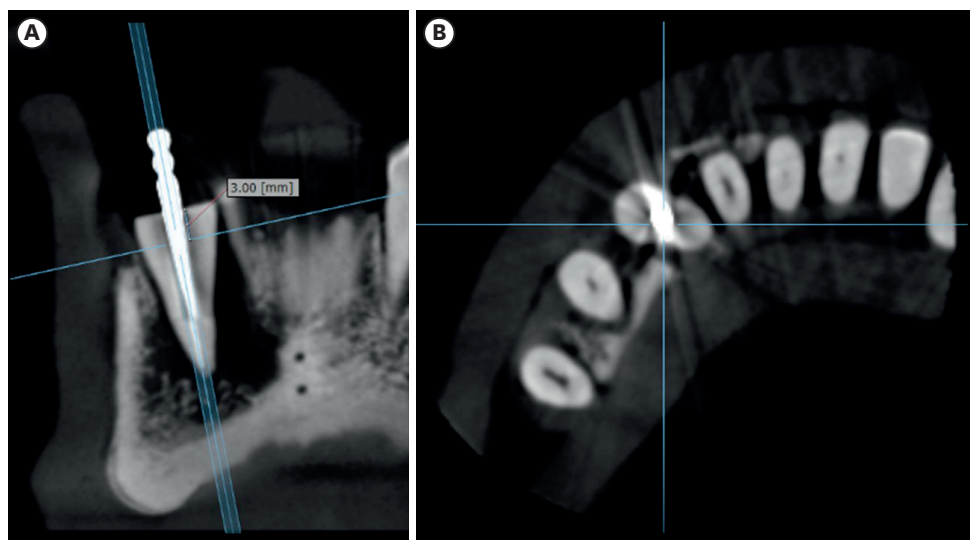


Figure 1. Obtaining the axial images used in the qualitative assessment of artifacts in all protocols. (A) Axial orientation line positioned 3 mm from the superior limit of the root and perpendicular to the root in an adjusted coronal reconstruction. (B) Axial reconstruction used in the template.

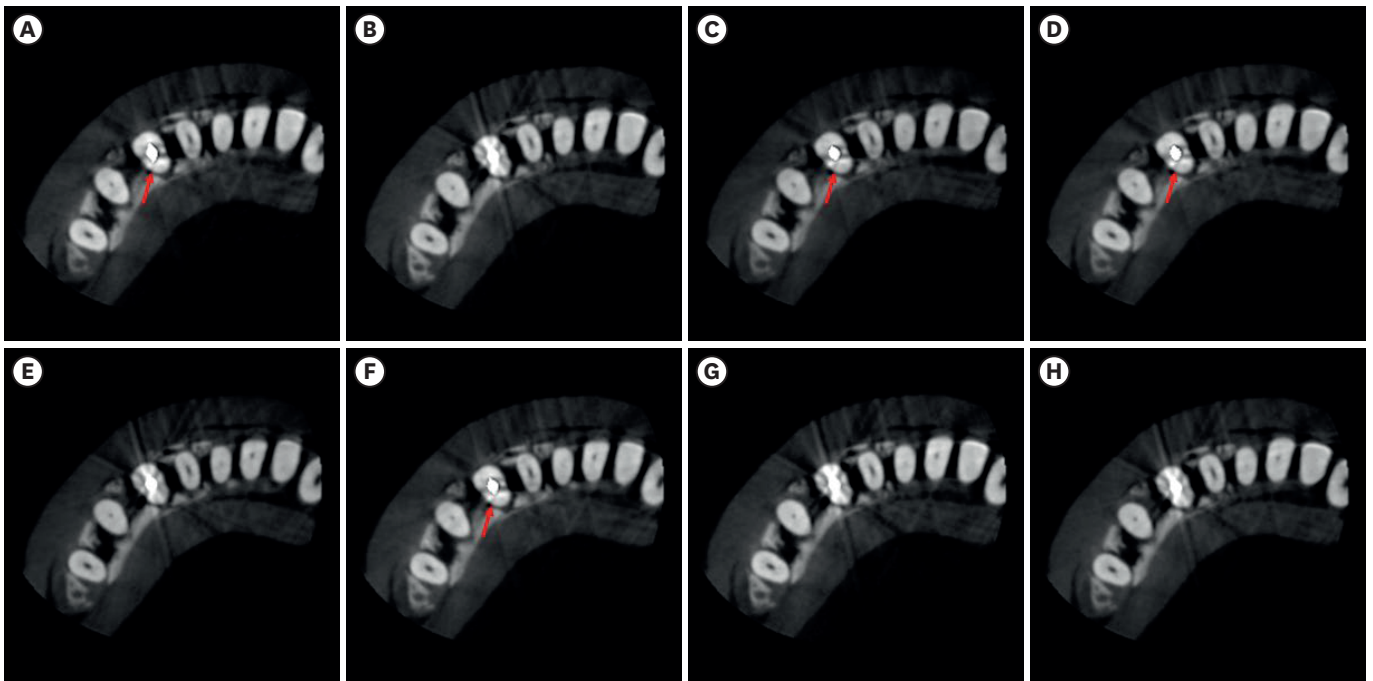


Figure 2. Example of the template used in the qualitative evaluation of artifacts. The images correspond to the axial reconstructions of the same tooth (of the group with vertical root fracture) obtained with all the studied protocols. (A) 70 kVp with MAR. (B) 80 kVp without MAR. (C) 99 kVp with MAR. (D) 90 kVp with MAR. (E) 99 kVp without MAR. (F) 80 kVp with MAR. (G) 70 kVp without MAR. (H) 90 kVp without MAR. The arrows indicate the fracture. kVp, peak kilovoltage; MAR, metal artifact reduction.

For the image quality evaluation scores (from 1 to 5), the median, mode, minimum, and maximum were calculated to express the results. The mode values of each protocol were used to compare the protocols using the Friedman test. The mode was chosen because it represented the response of the most examiners.

For the subjective assessment of the quantity of artifacts, when examiners assigned scores from 1 to 8 by comparing the axial images, all examiners' responses were analyzed descriptively and used to construct a graph to show the sum of responses for each protocol.

To evaluate intra- and inter-examiner reproducibility, the weighted kappa test was used, and the results were analyzed according to Landis and Koch [16].

RESULTS

Table 1 shows the mean values of the area under the ROC curve, sensitivity, and specificity of the VRF diagnosis. Neither kVp nor MAR influenced the diagnosis of VRF ($p > 0.05$).

Table 2 shows the median, mode, minimum, and maximum of the scores attributed by the examiners in the evaluation of image quality. In general, increasing the kVp and using MAR improved image scores. The Friedman test showed that scans acquired with 70 kVp without MAR received worse scores than those acquired with MAR regardless of the kVp, and scans of 99 kVp with MAR received higher scores than scans without MAR regardless of the kVp ($p < 0.05$).

Table 1. Mean values (and standard deviation) for the area under the receiver operating characteristic curve (AUC), sensitivity, and specificity for the diagnosis of vertical root fracture

Diagnostic test	kVp	Without MAR	With MAR	p value for kVp	p value for MAR	p value for interaction
AUC	70	0.634 (0.023)	0.692 (0.132)	0.053	0.856	0.458
	80	0.582 (0.057)	0.537 (0.130)			
	90	0.565 (0.081)	0.585 (0.051)			
	99	0.658 (0.108)	0.605 (0.074)			
Sensitivity	70	0.340 (0.219)	0.420 (0.164)	0.817	0.367	0.974
	80	0.280 (0.192)	0.375 (0.222)			
	90	0.320 (0.192)	0.340 (0.114)			
	99	0.380 (0.295)	0.420 (0.179)			
Specificity	70	0.780 (0.249)	0.880 (0.164)	0.936	0.094	0.237
	80	0.880 (0.130)	0.700 (0.216)			
	90	0.860 (0.152)	0.740 (0.134)			
	99	0.920 (0.179)	0.740 (0.114)			

kVp, peak kilovoltage; MAR, metal artifact reduction.

Table 2. Scores assigned in the evaluation of image quality

MAR	kVp	Median	Mode	Minimum	Maximum
Without	70*	2	2	1	4
	80	2	2	1	4
	90	3	2	1	4
	99	3	2	1	5
With	70	3	3	1	5
	80	3	3	1	5
	90	3	4	2	5
	99†	3	4	2	5

*70 kVp without MAR significantly differed from those protocols with MAR regardless of the kVp.

†99 kVp with MAR significantly differed from those protocols without MAR regardless of the kVp.

1, very poor; 2, poor; 3, acceptable; 4, good; 5, excellent.

kVp, peak kilovoltage; MAR, metal artifact reduction.

In the subjective assessment of the artifact expression, the images obtained from the protocol with 99 kVp were scored as the best (i.e., the fewest artifacts) in most cases; conversely, the protocol with 70 kVp was the worst, especially in the absence of MAR. All protocols obtained with the MAR tool received better scores than those obtained without MAR, regardless of kVp (Figure 3, left). Furthermore, the examiners' scores showed an increase in the artifact expression with a decrease in kVp in protocols with and without MAR.

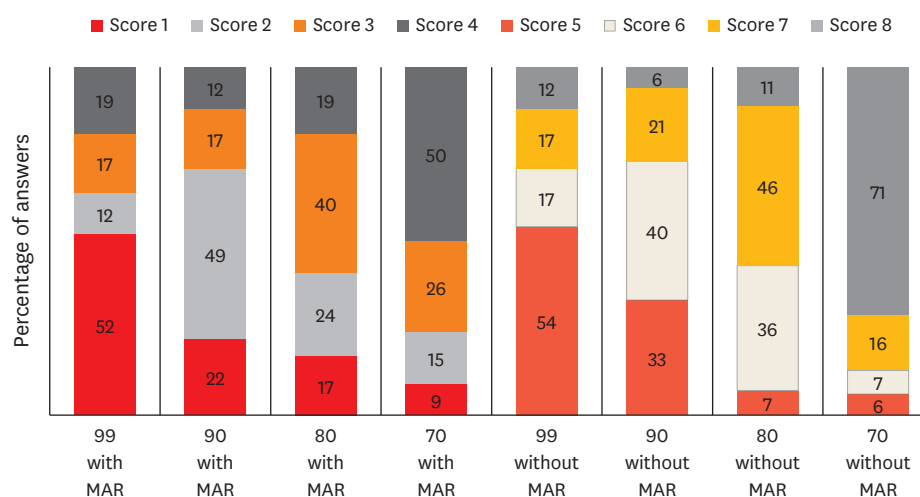


Figure 3. Distribution of the responses of the examiners for artifact expression in all protocols. kVp, peak kilovoltage; MAR, metal artifact reduction.

The weighted kappa test demonstrated that the intra-examiner agreement varied from slight to moderate for the diagnosis of VRF (0.094–0.464) and image quality (0.105–0.521), and from moderate to almost perfect for artifact expression (0.556–0.920). Inter-examiner agreement varied from slight to fair for the diagnosis of VRF (0.067–0.383) and image quality (0.042–0.385), and from moderate to almost perfect for artifact expression (0.549–0.913).

DISCUSSION

The detection of VRF in CBCT images is a challenge in clinical practice and becomes even more complex when the tooth has a high-atomic-number intracanal material, such as a metal post, due to the formation of artifacts [3]. Artifacts degrade the image quality, compromising the VRF diagnosis [1,4,17-19]. Thus, the objective of this study was to evaluate the influence of 2 parameters that directly affect the production of artifacts (kVp and the MAR tool) on the VRF diagnosis. Previous studies have already demonstrated the positive effect of these parameters on the reduction of artifacts when objectively assessed. Our hypothesis was that increasing the kVp in combination with the MAR tool could improve the diagnosis of VRF. However, no such effect was observed; therefore, the null hypothesis was accepted.

In fact, there is low scientific evidence regarding the impact of kVp in the diagnosis of VRF. Only 2 studies were found; however, one did not use intracanal metallic posts as a source of artifacts [4], precluding a direct comparison, and the other one used minimal kVp variation (70 and 74 kVp) [19]. Similarly to the present study, the last study found no influence of kVp on the diagnosis of VRF [19]; however, that could have been a result of the small variation in kVp in the protocols, hiding the real effect of kVp on VRF diagnosis. Conversely, in the present study, 4 levels of kVp were used. We expected that the larger difference among kVp levels would lead to different results from those observed in the previous study. Contrary to our expectations, we found that increasing the kVp did not improve the diagnostic accuracy, even with a larger kVp change. Therefore, these results reflect the negative impact of artifacts on VRF diagnosis, masking fracture lines and preventing fractures from being detected, which affects the sensitivity [20], without a positive effect of an increase in kVp.

It would be difficult to recommend a specific level of kVp to be used, since the choice should be based on the characteristics of the patient and CBCT device, as well as on the diagnostic task. Furthermore, kVp levels vary considerably among CBCT devices, ranging from 50 to 120 kVp [21], which also hinders a single recommendation. However, it is important that professionals be aware that increasing the kVp level up to 99 kVp did not improve the diagnostic accuracy of VRF.

It was observed that at all kVp levels, the specificity was higher than the sensitivity; therefore, we infer that the examiners assumed that most cases were free of VRF when the evaluation was complicated by the presence of artifacts. This result is significant because the reduction of false-positive results can prevent unnecessary extractions [22]. Another factor to be considered is the fracture configuration, which had no fragment separation [18,23-25].

The MAR tool was included in this study since it is an alternative method to reduce the expression of artifacts without increasing the radiation dose for the patient, as well as offering positive results for objective image quality [6,8,9,26]. In the present study, the subjective assessment of artifact expression showed better results for the images

obtained with the MAR tool than for those obtained without MAR. This indicates that the improvement in image quality found in studies that used objective analyses [8,13] was also observed subjectively. The graph showed a more significant influence of MAR than kVp on the scores assigned by the examiners.

However, this improvement seems to have had little or no influence on the VRF diagnosis, as observed in this and previous studies [16,27]. Bechara *et al.* [10] and Bezerra *et al.* [9] observed a negative impact of the MAR algorithm, once the accuracy and sensitivity decreased with the use of the algorithm. In contrast, Freitas *et al.* [4] observed an increase in specificity when using MAR; this difference can be attributed to the source of the artifacts studied being an implant close to the tooth instead of being caused by a filling material in the evaluated tooth.

The number of roots was based on previous studies with similar methodology [4,9,11,18], as it was considered sufficient to reach the diagnostic values. It is important to point out that in studies with this design, the most important factor is the number of examiners, since the dependent variables for the diagnosis of FRV are the diagnostic values (area under the ROC curve, sensitivity, and specificity) of each examiner, and not the number of roots. Furthermore, in the subjective analysis, the dependent variables were the scores attributed to each image by each examiner regarding the quality and expression of artifacts, totaling 100 responses for each protocol.

Ex vivo studies have the limitation of not considering all maxillofacial structures that influence the gray values on CBCT [9]. In addition, *ex vivo* studies do not allow the correlation of fractures with clinical findings, which can support the diagnosis [1]. However, an *in vivo* study would be impractical, as it would be unethical to acquire multiple CBCT examinations from the same patient. In this way, we simulated X-ray attenuation by soft tissues using utility wax covering the entire mandible, enabling images comparable to real scans. It should also be considered that only 1 CBCT device and 1 root filling material were used, which prohibits generalization of the results. The device was chosen because it allowed variation of the kVp level and MAR activation, independently of the other CBCT parameters. However, considering the variety of available CBCT devices and filling materials, further studies should be conducted.

The low intra- and inter-examiner agreement rates also deserve attention, as they could indicate doubts about the consistency of the evaluations and be considered as a limitation. However, these rates tend to be low in fracture studies, especially in the presence of metallic materials on CBCT [1,4,17,18], and our findings were similar to those previously reported. In the subjective evaluation of artifacts, the reproducibility was better because it did not include a diagnosis, but rather the examiners' opinion; this result showed that the examiners were consistent and well-trained.

Even though the diagnosis of VRF on CBCT is challenging, the American Association of Endodontics/ American Academy of Oral and Maxillofacial Radiology and European Society of Endodontology recommend CBCT examinations in cases of suspected VRF if a clinical examination and 2-dimensional radiography are inconclusive [28,29]. Since the kVp influences the radiation dose to the patient and its increase did not improve the diagnosis of VRF, increasing the kVp is not supported. Regarding MAR, although it has not shown clinical relevance for this diagnostic task, it made the images more subjectively acceptable

without changing the radiation dose. Considering that the activation of MAR increases the examination reconstruction time but does not change the radiation dose, it can be used according to the professional's preference.

CONCLUSIONS

Protocols with higher kVp combined with MAR improved the image quality in CBCT scans when subjectively analyzed. However, these factors did not improve the diagnosis of VRF. Professionals should be aware of these factors when selecting a CBCT protocol.

ACKNOWLEDGEMENTS

The authors would like to thank the examiners.

REFERENCES

1. Ferreira LM, Visconti MA, Nascimento HA, Dallemolle RR, Ambrosano GM, Freitas DQ. Influence of CBCT enhancement filters on diagnosis of vertical root fractures: a simulation study in endodontically treated teeth with and without intracanal posts. *Dentomaxillofac Radiol* 2015;44:20140352. [PUBMED](#) | [CROSSREF](#)
2. Yamamoto-Silva FP, de Oliveira Siqueira CF, Silva MA, Fonseca RB, Santos AA, Estrela C, de Freitas Silva BS. Influence of voxel size on cone-beam computed tomography-based detection of vertical root fractures in the presence of intracanal metallic posts. *Imaging Sci Dent* 2018;48:177-184. [PUBMED](#) | [CROSSREF](#)
3. Chang E, Lam E, Shah P, Azarpazhooh A. Cone-beam computed tomography for detecting vertical root fractures in endodontically treated teeth: a systematic review. *J Endod* 2016;42:177-185. [PUBMED](#) | [CROSSREF](#)
4. Freitas DQ, Vasconcelos TV, Noujeim M. Diagnosis of vertical root fracture in teeth close and distant to implant: an in vitro study to assess the influence of artifacts produced in cone beam computed tomography. *Clin Oral Investig* 2019;23:1263-1270. [PUBMED](#) | [CROSSREF](#)
5. Schulze R, Heil U, Gross D, Bruellmann DD, Dranischnikow E, Schwanecke U, Schoemer E. Artefacts in CBCT: a review. *Dentomaxillofac Radiol* 2011;40:265-273. [PUBMED](#) | [CROSSREF](#)
6. Queiroz PM, Oliveira ML, Groppo FC, Haiter-Neto F, Freitas DQ. Evaluation of metal artefact reduction in cone-beam computed tomography images of different dental materials. *Clin Oral Investig* 2018;22:419-423. [PUBMED](#) | [CROSSREF](#)
7. Bechara BB, Moore WS, McMahan CA, Noujeim M. Metal artefact reduction with cone beam CT: an *in vitro* study. *Dentomaxillofac Radiol* 2012;41:248-253. [PUBMED](#) | [CROSSREF](#)
8. Helvacioğlu-Yigit D, Demirtürk Kocasarac H, Bechara B, Noujeim M. Evaluation and reduction of artifacts generated by 4 different root-end filling materials by using multiple cone-beam computed tomography imaging settings. *J Endod* 2016;42:307-314. [PUBMED](#) | [CROSSREF](#)
9. Bezerra IS, Neves FS, Vasconcelos TV, Ambrosano GM, Freitas DQ. Influence of the artefact reduction algorithm of Picasso Trio CBCT system on the diagnosis of vertical root fractures in teeth with metal posts. *Dentomaxillofac Radiol* 2015;44:20140428. [PUBMED](#) | [CROSSREF](#)
10. Bechara B, Alex McMahan C, Moore WS, Noujeim M, Teixeira FB, Geha H. Cone beam CT scans with and without artefact reduction in root fracture detection of endodontically treated teeth. *Dentomaxillofac Radiol* 2013;42:20120245. [PUBMED](#) | [CROSSREF](#)

11. de Rezende Barbosa GL, Sousa Melo SL, Alencar PN, Nascimento MC, Almeida SM. Performance of an artefact reduction algorithm in the diagnosis of in vitro vertical root fracture in four different root filling conditions on CBCT images. *Int Endod J* 2016;49:500-508.
[PUBMED](#) | [CROSSREF](#)
12. Pauwels R, Araki K, Siewerdsen JH, Thongvigitmanee SS. Technical aspects of dental CBCT: state of the art. *Dentomaxillofac Radiol* 2015;44:20140224.
[PUBMED](#) | [CROSSREF](#)
13. Freitas DQ, Fontenele RC, Nascimento EH, Vasconcelos TV, Noujeim M. Influence of acquisition parameters on the magnitude of cone beam computed tomography artifacts. *Dentomaxillofac Radiol* 2018;47:20180151.
[PUBMED](#) | [CROSSREF](#)
14. Oliveira ML, Freitas DQ, Ambrosano GM, Haiter-Neto F. Influence of exposure factors on the variability of CBCT voxel values: a phantom study. *Dentomaxillofac Radiol* 2014;43:20140128.
[PUBMED](#) | [CROSSREF](#)
15. Vasconcelos TV, Bechara BB, McMahan CA, Freitas DQ, Noujeim M. Evaluation of artifacts generated by zirconium implants in cone-beam computed tomography images. *Oral Surg Oral Med Oral Pathol Oral Radiol* 2017;123:265-272.
[PUBMED](#) | [CROSSREF](#)
16. Landis JR, Koch GG. The measurement of observer agreement for categorical data. *Biometrics* 1977;33:159-174.
[PUBMED](#) | [CROSSREF](#)
17. Hassan B, Metska ME, Ozok AR, van der Stelt P, Wesselink PR. Comparison of five cone beam computed tomography systems for the detection of vertical root fractures. *J Endod* 2010;36:126-129.
[PUBMED](#) | [CROSSREF](#)
18. Neves FS, Freitas DQ, Campos PS, Ekestubbe A, Lofthag-Hansen S. Evaluation of cone-beam computed tomography in the diagnosis of vertical root fractures: the influence of imaging modes and root canal materials. *J Endod* 2014;40:1530-1536.
[PUBMED](#) | [CROSSREF](#)
19. Pinto MG, Rabelo KA, Sousa Melo SL, Campos PS, Oliveira LS, Bento PM, Melo DP. Influence of exposure parameters on the detection of simulated root fractures in the presence of various intracanal materials. *Int Endod J* 2017;50:586-594.
[PUBMED](#) | [CROSSREF](#)
20. Gaêta-Araujo H, Silva de Souza GQ, Freitas DQ, de Oliveira-Santos C. Optimization of tube current in cone-beam computed tomography for the detection of vertical root fractures with different intracanal materials. *J Endod* 2017;43:1668-1673.
[PUBMED](#) | [CROSSREF](#)
21. Gaêta-Araujo H, Alzoubi T, Vasconcelos KF, Orhan K, Pauwels R, Casselman JW, Jacobs R. Cone beam computed tomography in dentomaxillofacial radiology: a two-decade overview. *Dentomaxillofac Radiol* 2020;49:20200145.
[PUBMED](#) | [CROSSREF](#)
22. Codari M, de Faria Vasconcelos K, Ferreira Pinheiro Nicolielo L, Haiter Neto F, Jacobs R. Quantitative evaluation of metal artifacts using different CBCT devices, high-density materials and field of views. *Clin Oral Implants Res* 2017;28:1509-1514.
[PUBMED](#) | [CROSSREF](#)
23. Brady E, Mannocci F, Brown J, Wilson R, Patel S. A comparison of cone beam computed tomography and periapical radiography for the detection of vertical root fractures in nonendodontically treated teeth. *Int Endod J* 2014;47:735-746.
[PUBMED](#) | [CROSSREF](#)
24. Makeeva IM, Byakova SF, Novozhilova NE, Adzhieva EK, Golubeva GI, Grachev VI, Kasatkina IV. Detection of artificially induced vertical root fractures of different widths by cone beam computed tomography *in vitro* and *in vivo*. *Int Endod J* 2016;49:980-989.
[PUBMED](#) | [CROSSREF](#)
25. Zhang L, Wang T, Cao Y, Wang C, Tan B, Tang X, Tan R, Lin Z. *In vivo* detection of subtle vertical root fracture in endodontically treated teeth by cone-beam computed tomography. *J Endod* 2019;45:856-862.
[PUBMED](#) | [CROSSREF](#)
26. Bechara B, McMahan CA, Geha H, Noujeim M. Evaluation of a cone beam CT artefact reduction algorithm. *Dentomaxillofac Radiol* 2012;41:422-428.
[PUBMED](#) | [CROSSREF](#)
27. Dalili Kajan Z, Taramsari M, Khosravi Fard N, Khaksari F, Moghasem Hamidi F. The efficacy of metal artifact reduction mode in cone-beam computed tomography images on diagnostic accuracy of root fractures in teeth with intracanal posts. *Iran Endod J* 2018;13:47-53.
[PUBMED](#)

28. Special Committee to Revise the Joint AAE/AAOMR Position Statement on use of CBCT in Endodontics. AAE and AAOMR joint position statement: use of cone beam computed tomography in endodontics 2015 update. Oral Surg Oral Med Oral Pathol Oral Radiol 2015;120:508-512.
[PUBMED](#) | [CROSSREF](#)
29. Patel S, Brown J, Semper M, Abella F, Mannocci F. European Society of Endodontology position statement: use of cone beam computed tomography in Endodontics: European Society of Endodontology (ESE) developed by. Int Endod J 2019;52:1675-1678.
[PUBMED](#) | [CROSSREF](#)